First geoneutrino measurement in JUNO

Qishan Liu 刘琪汕
(on behalf of the JUNO Collaboration)
Institute of High Energy Physics

Content

Neutrino

The ghostly messengers of the universe

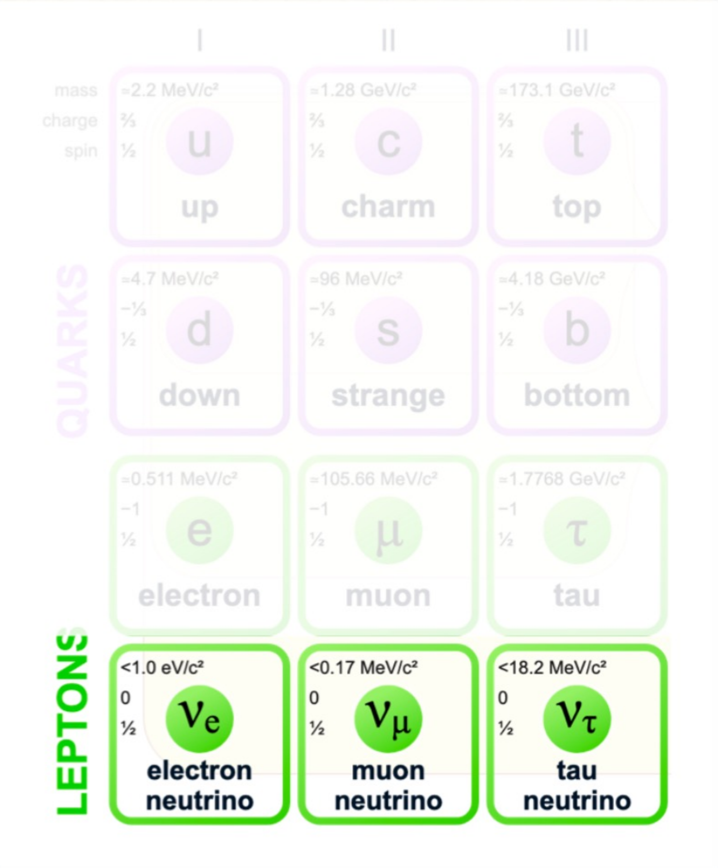

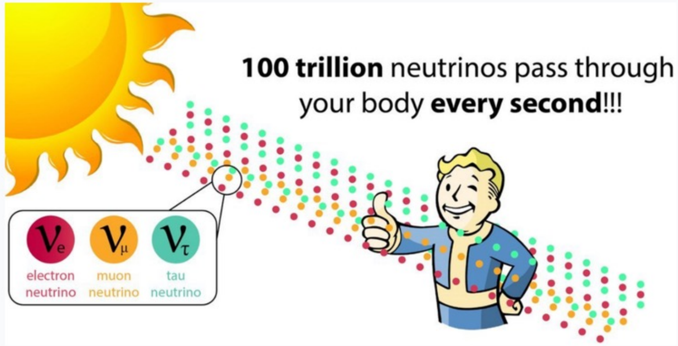

- Neutrinos in the Standard Model — three flavors paired with charged leptons
- Second most abundant particle in the universe
- Interact only via the weak force and gravity

  → Unique astronomical messengers from the densest environments
- Extremely small interaction cross sections

  → Very low event rates in any detector

Neutrino Oscillation

$$|\nu_\alpha\rangle = \sum_{i=1}^{3} U^*_{\alpha i}|\nu_i\rangle$$

- Neutrinos propagate as **mass eigenstates** but are produced/ detected as **flavor eigenstates**
- Flavor change arises from the mismatch between the two bases — described by the **PMNS matrix**
- Governed by 3 mixing angles $(\theta_{12}, \theta_{23}, \theta_{13})$, 2 mass-squared differences, CP phase

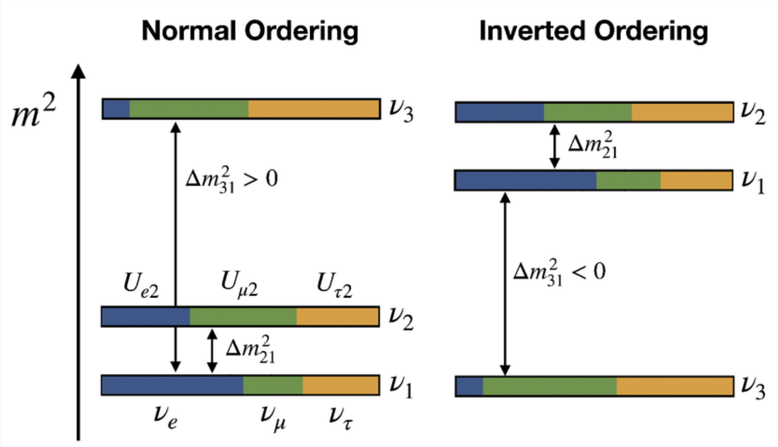

Open questions:

- Neutrino Mass Ordering (NMO)
- Absolute mass
- Origin of neutrino mass
- CP-violating phase
- Dirac vs Majorana
- Existence of sterile neutrino

...

Neutrino Sources

A multi-purpose detector for neutrino physics

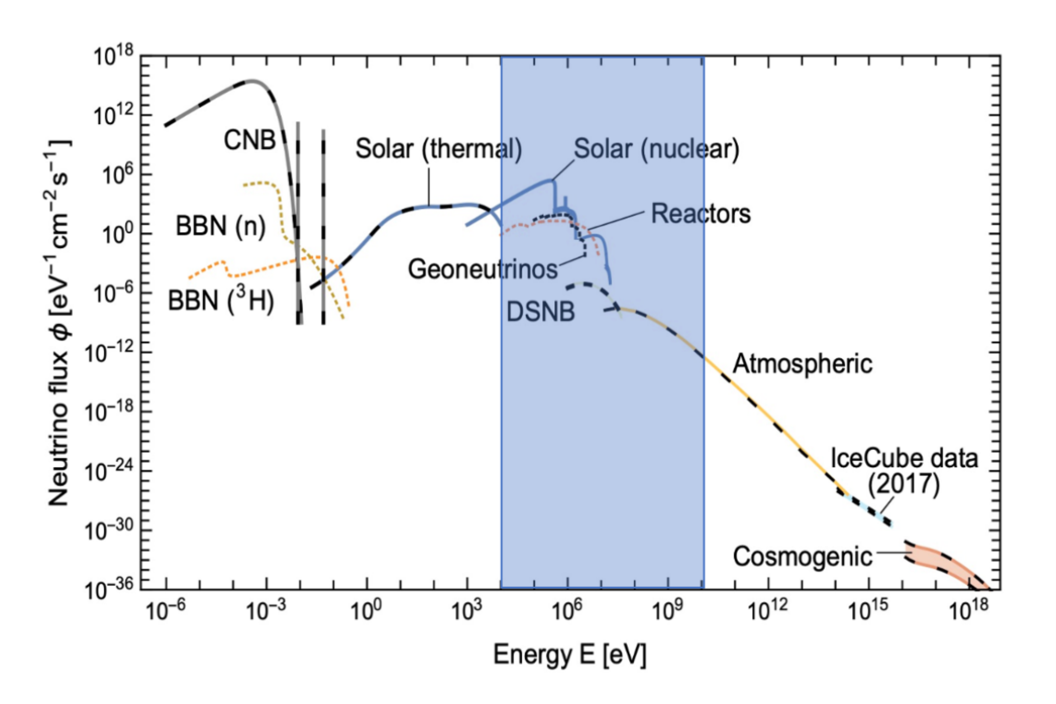

Neutrino sources accessible to JUNO: reactor, solar, geoneutrino, atmospheric, DSNB, supernova

JUNO — Key Capabilities

- **20,000 ton** liquid-scintillator detector
- Excellent energy resolution
- Wide energy range
- Low background levels

Beyond its primary physics goals, JUNO is a truly **multi-purpose detector** — spanning NMO, oscillation precision, solar physics, geoneutrinos, supernova, DSNB, and BSM searches.

Detection Channel — Inverse Beta Decay

The golden channel for MeV-scale $\bar{\nu}_e$

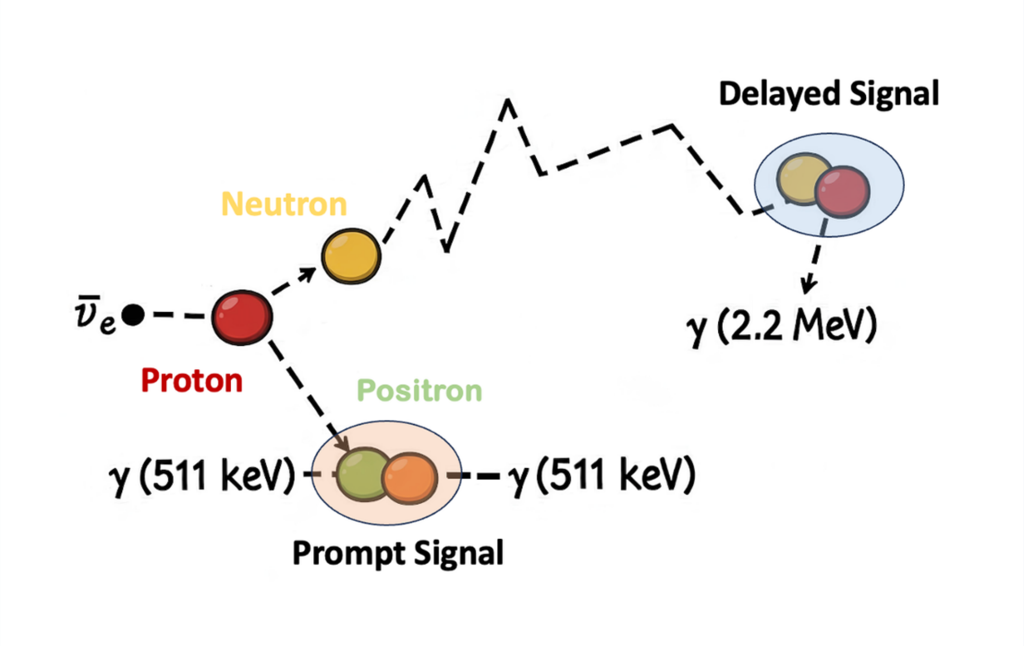

IBD reaction: prompt positron + delayed neutron capture

$$\bar{\nu}_e + p \to e^+ + n$$

- **Charged-current** interaction mediated by W boson
- Sensitive only to **electron flavour**
- Cross section well known
- **Threshold = 1.806 MeV** · Geoneutrino end-point ~ 3.3 MeV

Prompt-delayed signature:
- **Prompt**: e^+ deposits kinetic energy + annihilates $\to 2\gamma$
- **Delayed** ($\sim 200\ \mu$s): n thermalizes, captured on H (~99%) or ^{12}C (~1%) ⇒ 2.223 MeV γ (H) or 4.95 MeV γ (^{12}C)

⇒ Tight space–time coincidence = *powerful background suppression*

JUNO Location & Primary Goal

Optimized baseline for the Neutrino Mass Ordering

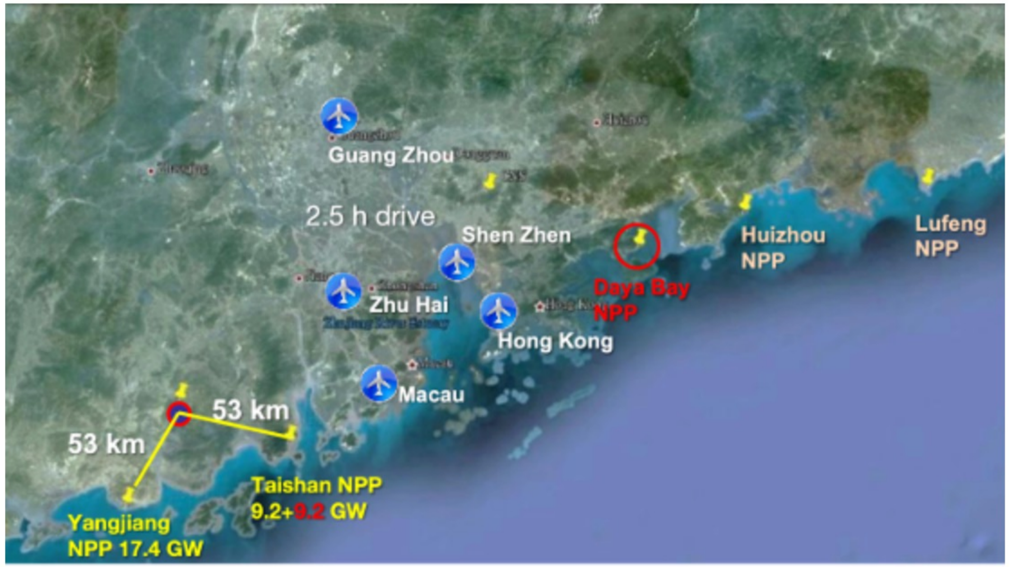

Primary physics goal: determine the *Neutrino Mass Ordering*
— normal ($m_1 < m_2 < m_3$) vs inverted ($m_3 < m_1 < m_2$)
— independent of matter effects & CP phase

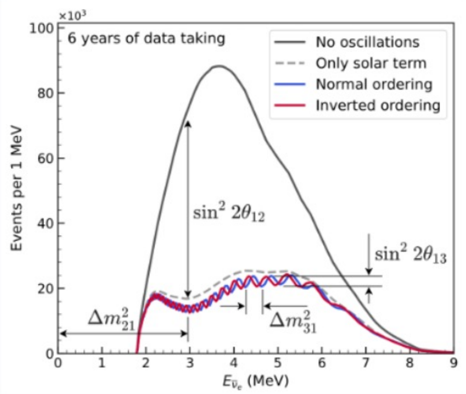

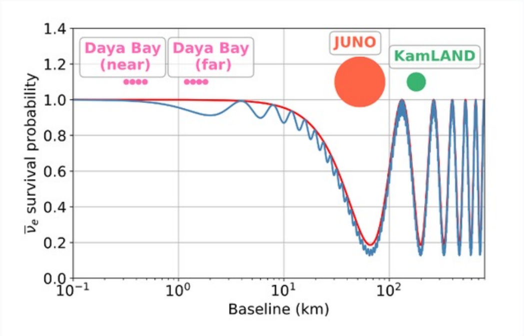

- Located in Jiangmen, Guangdong — 650 m rock overburden
- 52.5 km from the Yangjiang & Taishan reactor
- Equidistant from both ⇒ effectively doubles the neutrino flux
- Sits at the first solar oscillation maximum ⇒ maximal spectral distortion

The JUNO Detector

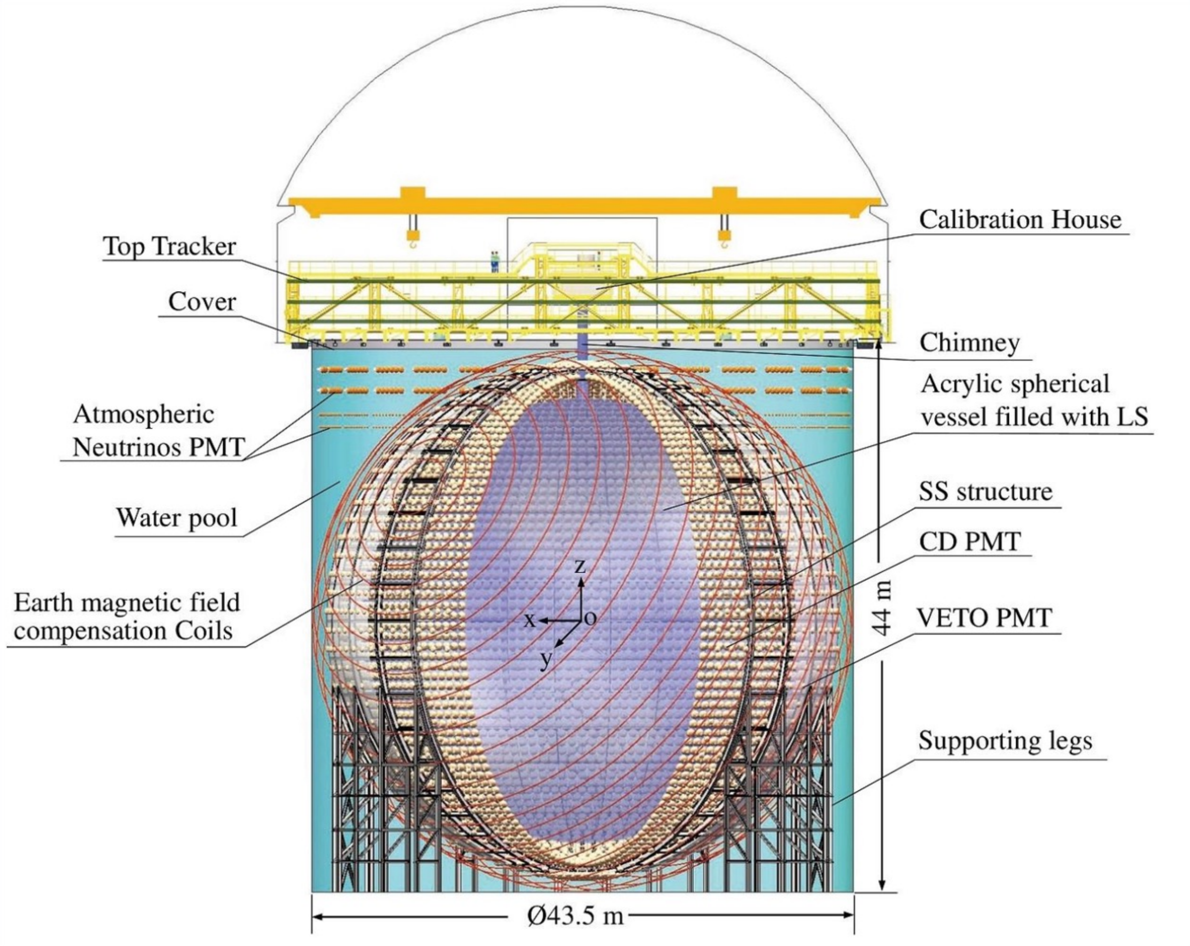

VETO System

- Top Tracker — plastic scintillator
- Water Pool: Ø43.5 m, H 44 m
- Earth magnetic-field shielding coils

Central Detector

- Stainless-steel structure · 35.4 m Ø acrylic sphere
- **20 kton** LAB-based liquid scintillator
- 17,612 × 20″ PMT + 25,600 × 3″ PMT
- ⇒ 78% photocathode coverage · $3\%/\sqrt{E}$ resolution

Main Technical Challenges

- Precise mechanical structure for small clearance between PMTs
- Ultra-transparent LS (attenuation > 20 m)
- High photon efficiency PMTs

JUNO Detector Comparison

JUNO leads in target mass, light collection & energy resolution

Experiments	KamLAND	Borexino	SNO+	JUNO
Target Mass [tons]	1,000	300	780	**20,000**
Number of PMTs	~1,900	~2,200	~10,000	**17,612 + 25,600**
PMT Coverage	~34%	~30%	~50%	**78%**
Light Collection [p.e./MeV]	~250	~450	~520	**> 1,600**
Energy Resolution	$6\%/\sqrt{E}$	$5\%/\sqrt{E}$	$5\%/\sqrt{E}$	$3\%/\sqrt{E}$

JUNO's **20 kton target** + $3\%/\sqrt{E}$ energy resolution make it the world's most sensitive geoneutrino detector.

IBD Event Selection

Prompt–delayed coincidence in time, space & energy

Criterion	Selection
PMT flasher	Applied
Fiducial volume	r_p < 17.2 m, $\|z_p\|$<15.5m
Prompt energy	(0.7, 12) MeV
Delayed energy	(2.0, 2.5) ∪ (4.5, 5.5) MeV
Coincidence time	(5, 1000) μs
Relative distance	< 1.5 m
Multiplicity cut	No other events > 0.7 MeV in the FV or (2.0, 6.0) MeV outside the FV within 2 ms before and 1 ms after the delayed event
Water pool muon veto	Veto if the delayed is within (0, 2) ms after NPE > 700 in WP
CD muon veto	Veto if the delayed is within (0, 5) ms after NPE > 3×10^4 in CD
Spallation neutron veto	Veto if the delayed satisfies Δr < 4 m and Δt < 1.2 s after spallation neutrons with $NPE_{spn} \in (3000, 30000)$ and $T_{spn2\mu} \in (20, 2000)$ μs
Muon track veto	Veto if the delayed event: $\frac{\Delta r_{\mu d}}{2.5m} + \frac{\Delta t_{\mu d}}{0.5s} < 1$
Correlated discriminator	log(L.R.) > -1.26

Selection criteria

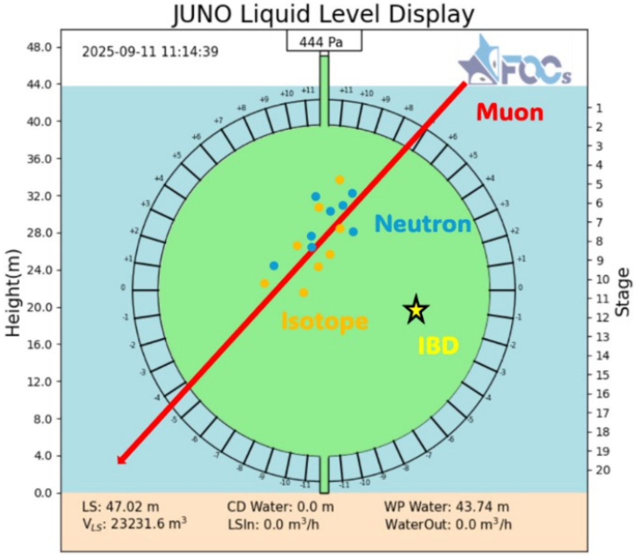

Muon veto

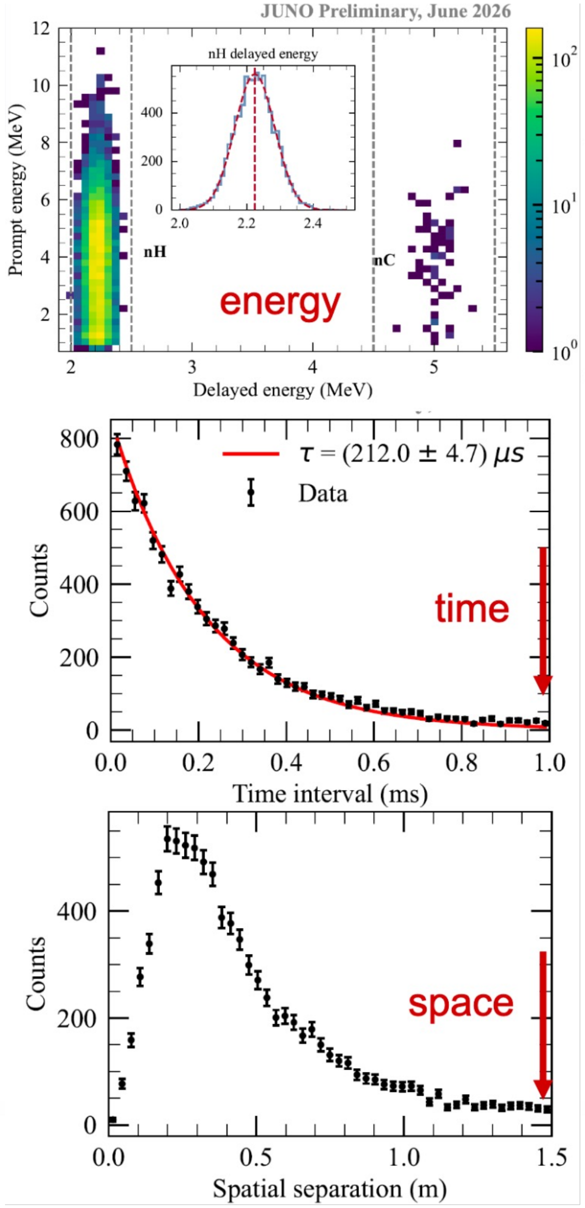

Neutrino Measurement in JUNO

Joint JUNO–TAO–Daya Bay spectral fit

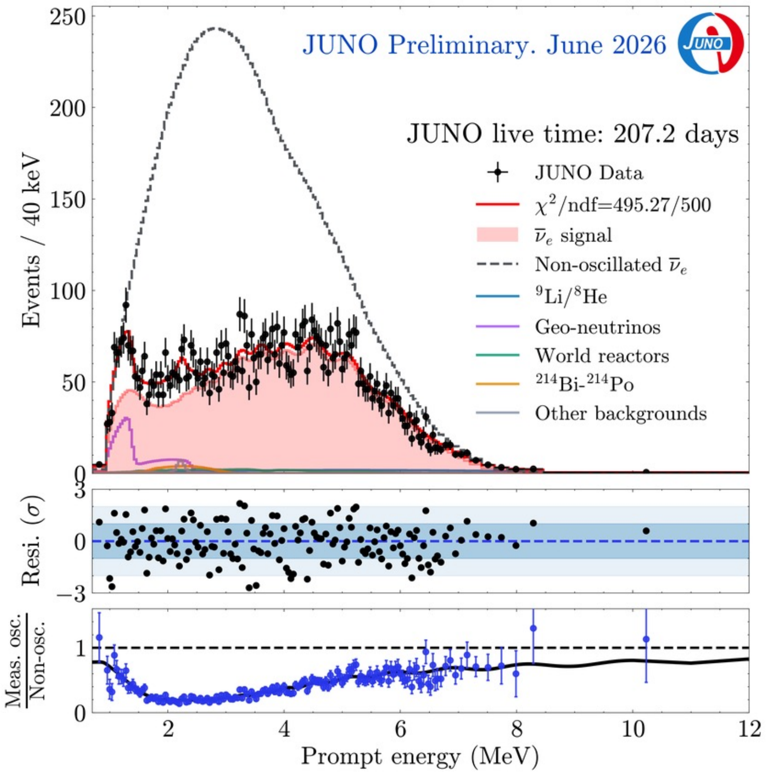

Antineutrinos ($\overline{\nu}_e$) Candidates Summary		
DAQ live time (days)	207.2	
$\overline{\nu}_e$ candidates	8294	
Selection Efficiencies (%)	ε	σ_{rel}
Fiducial volume	87.12%	0.96%
PMT flasher rejection	> 99.9%	Negligible
μ veto	93.67%	0.02%
Multiplicity cut	95.94%	negligible
Prompt-delayed coinc.	95.50%	0.32%
Correlated discriminator	98.99%	0.15%
Total efficiency (ε_{tot})	74.01%	1.02%
$\overline{\nu}_e$ **signal (cpd)**		
w/o ε_{tot} corrected	36.02 ± 0.62	
w/ ε_{tot} corrected	48.67 ± 1.08	
Backgrounds (cpd)	Pre-fit	Best-fit
^{9}Li/^{8}He	1.05 ± 0.27	1.41 ± 0.26
Geoneutrinos	Free	2.12
World reactors	0.92 ± 0.09	0.92 ± 0.09
^{214}Bi-^{214}Po	0.42 ± 0.31	0.57 ± 0.34
^{13}C(α, n)^{16}O	0.05 ± 0.02	0.05 ± 0.02
Fast neutrons	0.02 ± 0.02	0.02 ± 0.02
Double neutrons	0.10 ± 0.10	0.13 ± 0.10
Atmospheric neutrinos	0.09 ± 0.04	0.11 ± 0.05
Accidentals	0.07 ± 0.01	0.07 ± 0.01

- Reactor $\bar{\nu}_e$ flux constrained by
  - **TAO** satellite detector
  - **Daya Bay** near-detector data (PRL 130, 161802)

New Results of Solar Oscillation Parameters

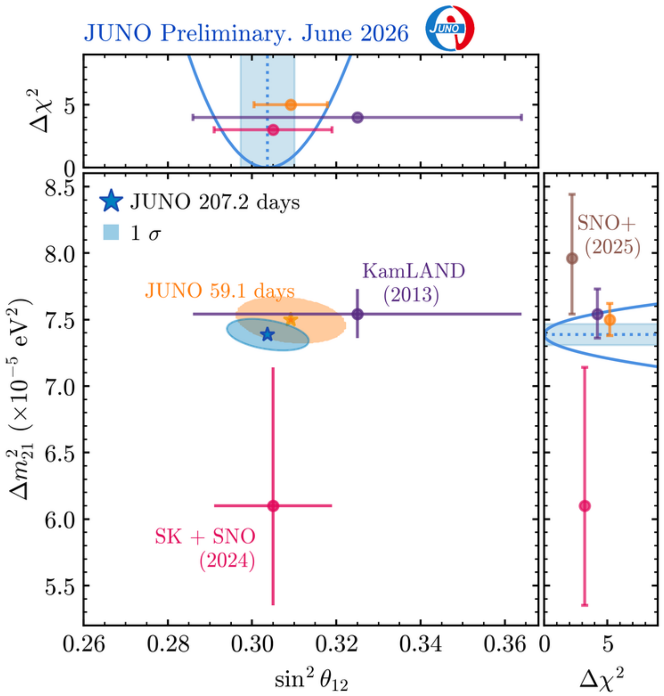

Parameter	JUNO best-fit	Precision (59.1 → 207.2 days)
Δm^2_{21}	7.388 ± 0.078	1.60% → **1.06%**
$\sin^2\theta_{12}$	0.3036 ± 0.0064	2.8% → **2.1%**

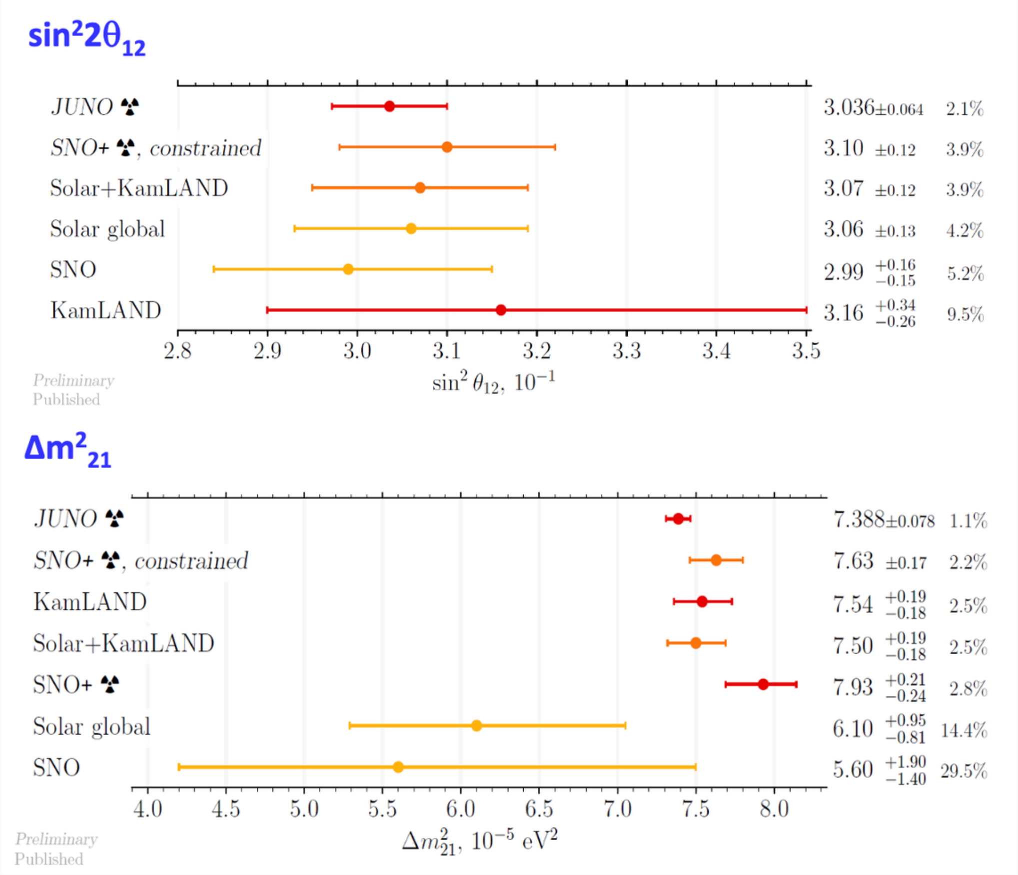

First Result of Δm^2_{31}

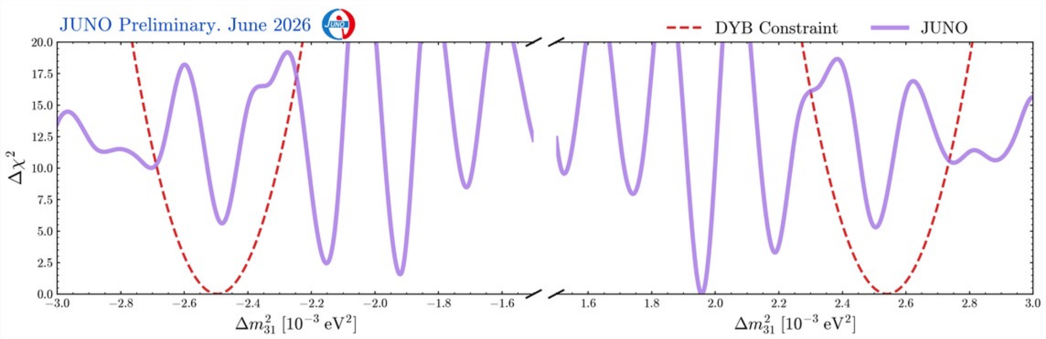

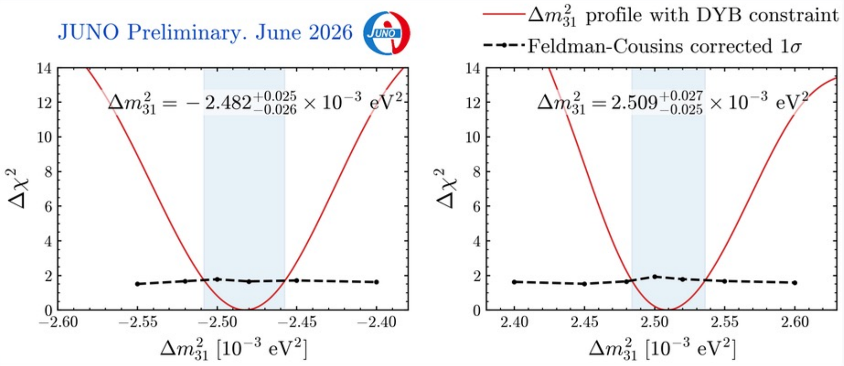

- The final minimum for each mass ordering is obtained by using the Δm^2_{31} constraint from **Daya Bay** (PRL 130 16, 161802)
- **Feldman–Cousins (FC)** method gives 1σ range of Δm^2_{31}: **~1% precision**

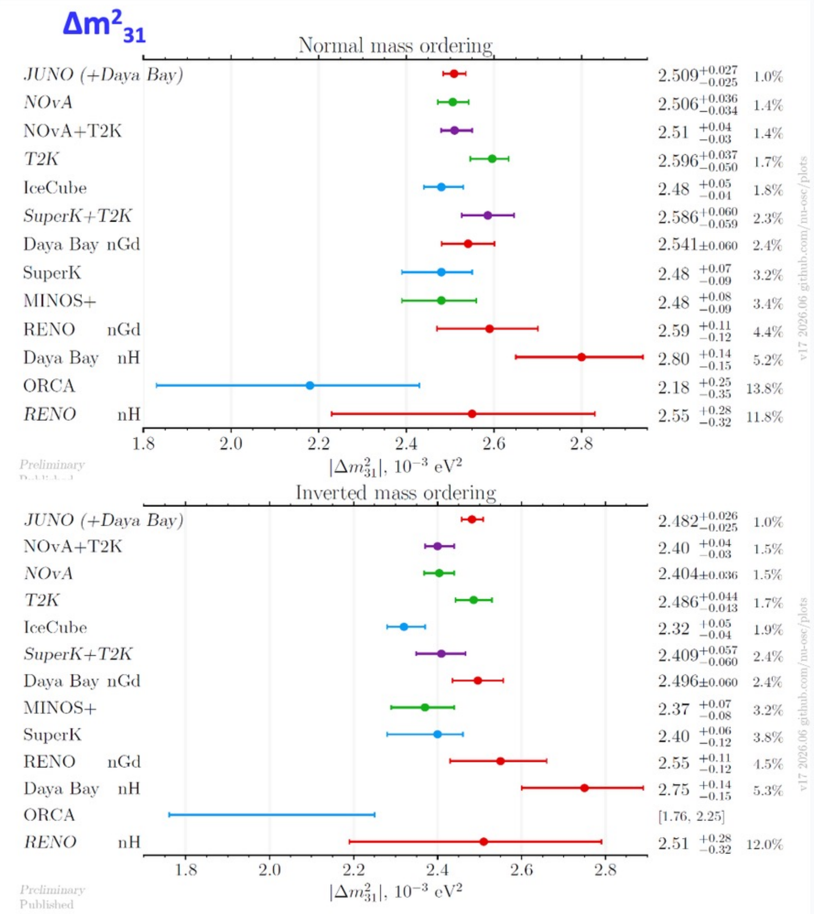

Adding Constraint from NuFit-LBL

- Δm^2_{31} from reactor and accelerator neutrinos should align at the right mass ordering[1]
- Adopt the NuFit-LBL results from [2]: **normal mass ordering is favored at $\Delta\chi^2 = 4.86$**

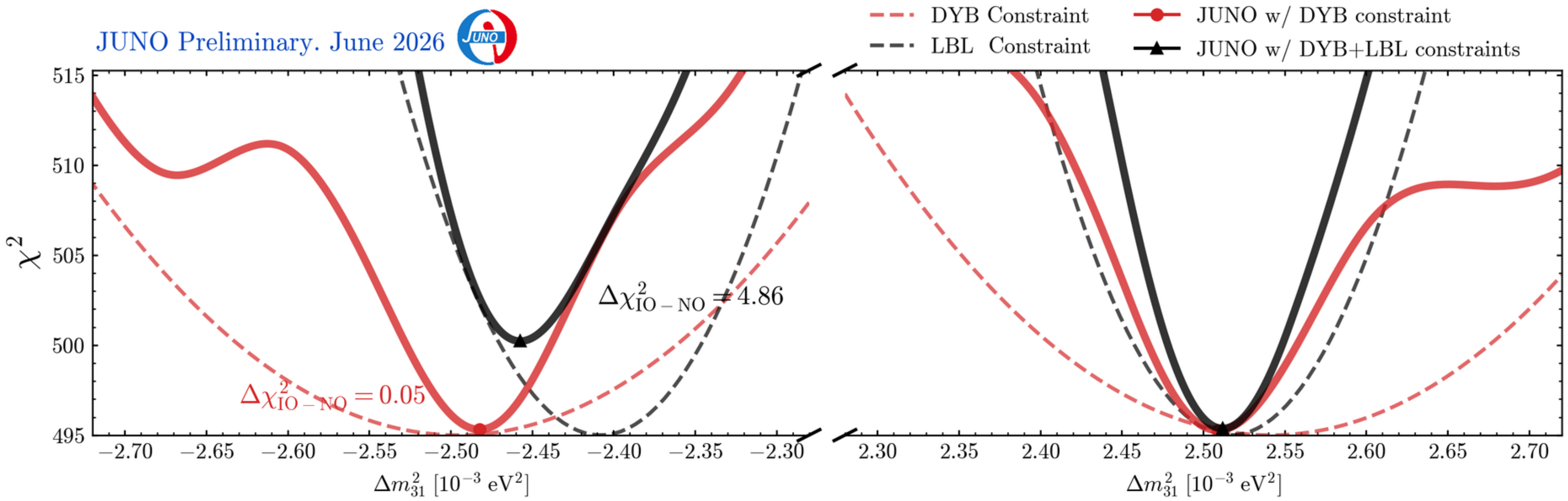

[1] H. Nunokawa, S. Parke and R. Z. Funchal, Phys. Rev. D 72 (2005) 013009; Y. F. Li et al., Phys. Rev. D 88, 013008 (2013)
[2] NuFIT 6.0 (JHEP 12 (2024) 216 [arXiv:2410.05380]), www.nu-fit.org, and M. Maltoni (private communication)

Neutrino Mass Ordering Significance

- **Frequentist** approach using pseudo-experiments to convert $\Delta\chi^2$ to significance
- Influence of δ_{CP} considered (scanned)
- **Normal Ordering** is favored at **2.3**σ

- **Bayesian** approach using Markov Chain Monte Carlo (MCMC) method
- Normal Ordering is favored with a Bayes factor of **10.18** $\Rightarrow 2\ln\kappa = 4.64$
- Consistent with the frequentist $\Delta\chi^2$

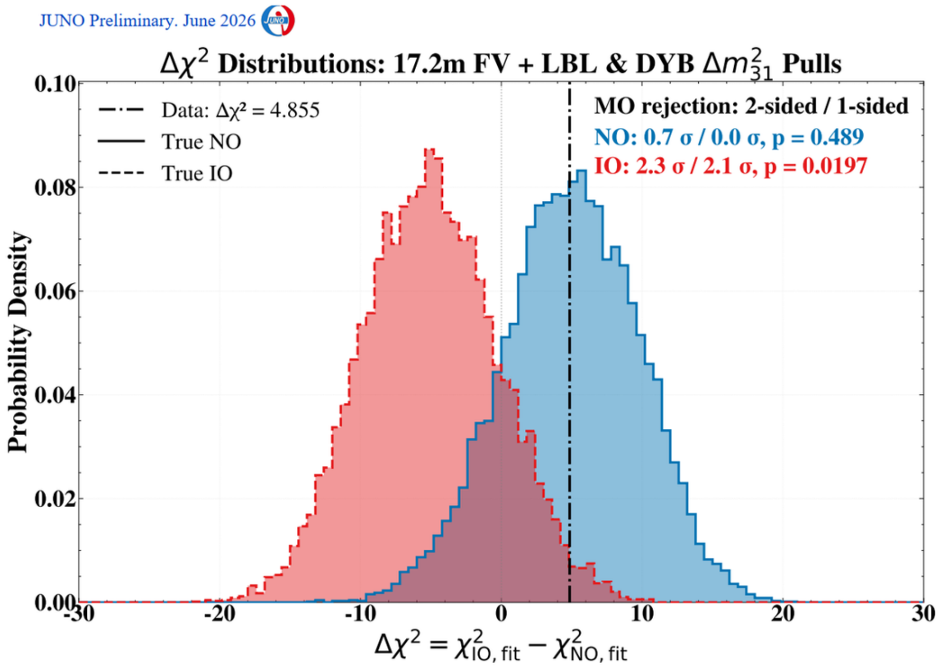

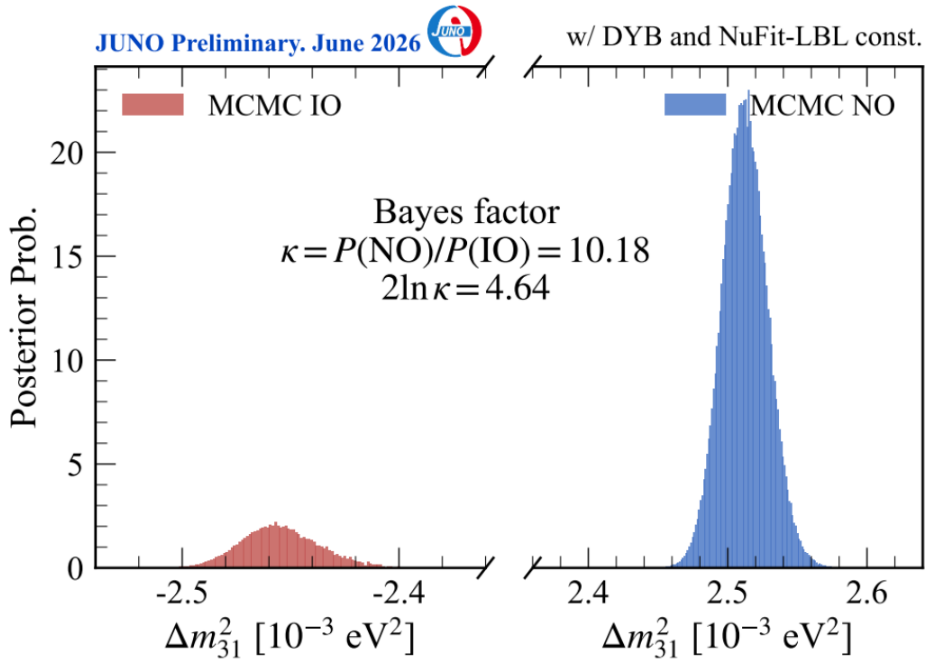

Geoneutrino Production & Spectra

From radioactive decays to detectable antineutrinos

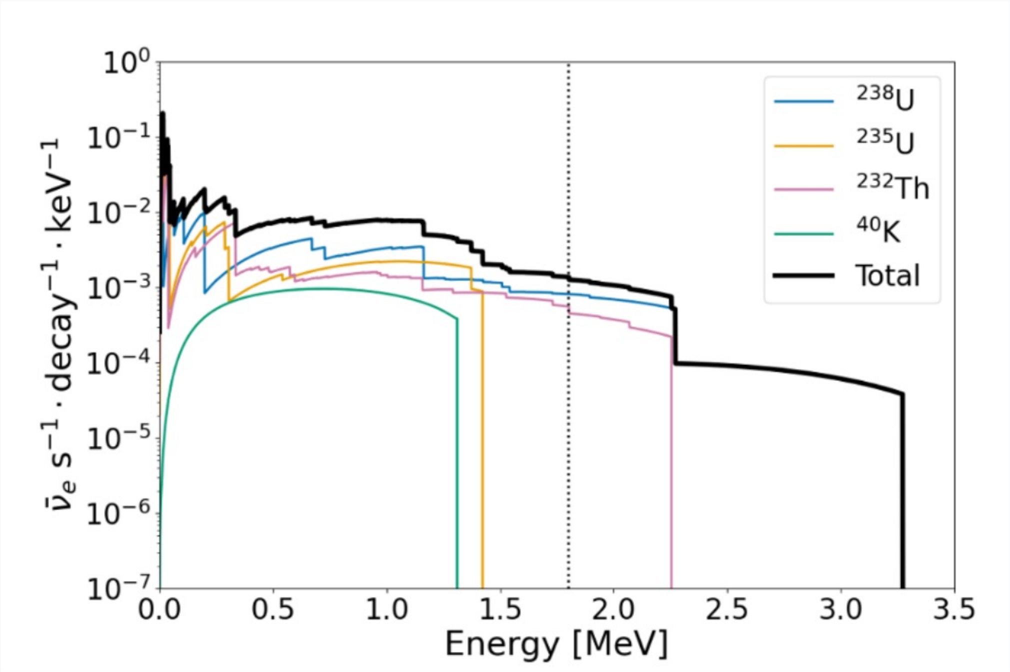

Geoneutrino energy spectra from ^{238}U, ^{235}U, ^{232}Th chains and ^{40}K. Vertical line: IBD threshold.

$$^{238}\mathrm{U} \rightarrow {}^{206}\mathrm{Pb} + 8\alpha + 6e^- + 6\bar{\nu}_e,\ \mathrm{Q} = 51.7\,\mathrm{MeV}$$
$$^{235}\mathrm{U} \rightarrow {}^{207}\mathrm{Pb} + 7\alpha + 4e^- + 4\bar{\nu}_e,\ \mathrm{Q} = 46.4\,\mathrm{MeV}$$
$$^{232}\mathrm{Th} \rightarrow {}^{208}\mathrm{Pb} + 6\alpha + 4e^- + 4\bar{\nu}_e,\ \mathrm{Q} = 42.6\,\mathrm{MeV}$$
$$^{40}\mathrm{K} \rightarrow {}^{40}\mathrm{Ca} + e^- + \bar{\nu}_e,\ \mathrm{Q} = 1.31\,\mathrm{MeV}\ (89.3\%)$$
$$^{40}\mathrm{K} + e^- \rightarrow {}^{40}\mathrm{Ar} + \nu_e,\ \mathrm{Q} = 1.504\,\mathrm{MeV}\ (10.7\%)$$

- Geoneutrinos from β-decays of **^{238}U, ^{235}U, ^{232}Th, ^{40}K** inside the Earth
- **Radiogenic heat** is in a well-known ratio to the number of emitted geoneutrinos
- IBD threshold $\Rightarrow$ only **^{238}U & ^{232}Th** detectable; ^{40}K below threshold
- Distinct spectral shapes enable **U/Th separation**

Geoneutrino

A direct probe of Earth's interior composition

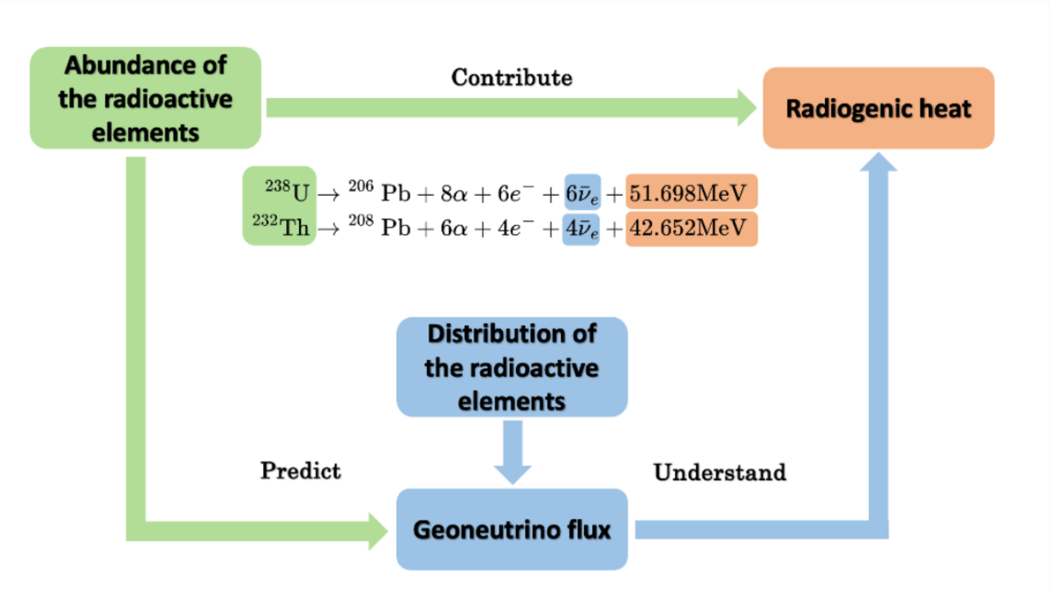

Geoneutrinos from U, Th, K decays throughout the Earth's crust and mantle

- Geoneutrino flux is **directly proportional** to the abundances of U and Th
- Their decays generate a **major fraction of Earth's radiogenic heat**
- **Direct constraints** on the terrestrial energy budget & interior structure

Geoneutrino Signal Component

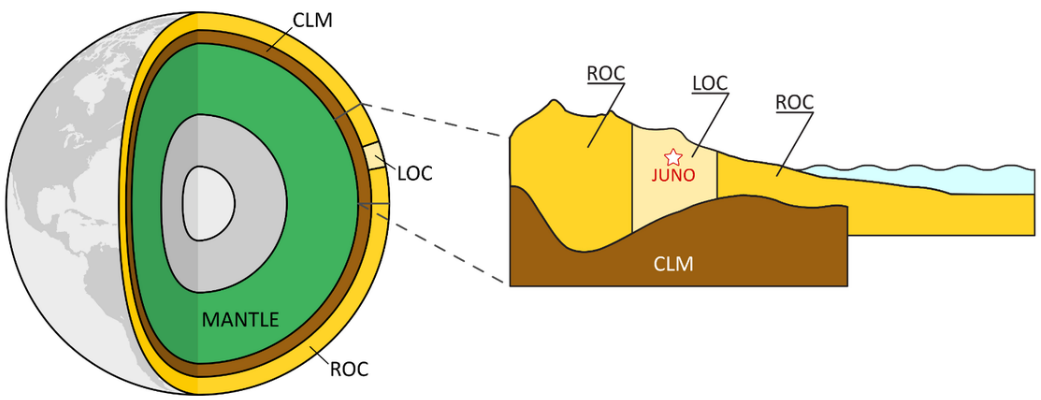

Earth's structure highlighting the components contributing to the geoneutrino signal.

- The **lithosphere** consists of the Earth's **crust** — split into the **Local Crust (LOC)** within a few hundred km of the detector and the **Rest of the Crust (ROC)** — plus the underlying **Continental Lithospheric Mantle (CLM)**.
- The experimental signal is the sum of two components: **mantle (M)** and **lithosphere (LS)**.
- The detector **cannot distinguish the neutrino direction**.
- To isolate the mantle contribution, the **lithosphere signal must be fixed and subtracted**.

Geoneutrino Signal Rate

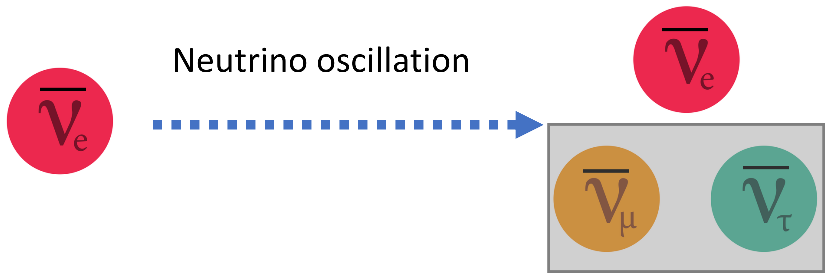

Abundances and density (g/cm^3) from geo models

Neutrino oscillation probability

Distance factor (g/cm^2)

$$f(i, E_{\bar{\nu}}) = \int P_{ee}\left(|\vec{r} - \vec{r}'|, E_{\bar{\nu}}\right) \cdot d^3r' \cdot \frac{a(i, \vec{r}') \cdot \rho(\vec{r}')}{4\pi |\vec{r} - \vec{r}'|^2}$$

Neutrino Flux (neutrino/s/cm^2)

$$\Phi_{osc}(i, \vec{r}) = \epsilon_{i,\bar{\nu}} \cdot \int dE_{\bar{\nu}} \cdot \mathrm{Sp}(i, E_{\bar{\nu}}) \cdot f(i, E_{\bar{\nu}})$$

Neutrino production rate (Neutrino/s/g)

Neutrino spectrum (/MeV)

Neutrino Signal

$$R[\mathrm{TNU}] = 10^{32} \cdot \frac{\text{seconds}}{\text{year}} \cdot \epsilon_{i,\bar{\nu}} \cdot \int dE_{\bar{\nu}} \cdot Sp(i, E_{\bar{\nu}}) \cdot \sigma_{\mathrm{IBD}}(i, E_{\bar{\nu}}) \cdot f(i, E_{\bar{\nu}})$$

IBD events per 10^{32} free protons per year

IBD cross section (cm^2)

Lithospheric and Mantle Models

Predicted geoneutrino signal contributions at JUNO

Lithospheric Models

Model	LOC Area (L×Lat)	S(U+Th) [TNU]
RRM	$6^\circ \times 4^\circ$	$30.9^{+6.5}_{-5.2}$
GIGJ	$6^\circ \times 4^\circ$	$28.9^{+5.5}_{-4.4}$
W20 [Crust 2.0]	$6^\circ \times 4^\circ$	$32.0^{+8.2}_{-6.6}$
W20 [Crust 1.0]	$6^\circ \times 4^\circ$	$31.7^{+8.4}_{-6.6}$
W20 [Litho 1.0]	$6^\circ \times 4^\circ$	$30.7^{+8.1}_{-6.4}$
JULOC	$10^\circ \times 10^\circ$	$40.4^{+5.6}_{-5.0}$
JULOC-I	$10^\circ \times 10^\circ$	$41.2^{+4.6}_{-3.3}$

Mantle Models (BSE classes)

BSE Class	S_{M}(U+Th) [TNU]
Poor-H	$2.8^{+2.4}_{-1.9}$
Medium-H	$8.0^{+4.0}_{-3.2}$
Rich-H	$17.4^{+5.7}_{-4.7}$

Global models give $S_{\mathrm{LS}} \approx 29$–$32$ TNU (~20% uncertainty), while the **local JULOC** models predict a markedly higher signal of ~ 40–41 TNU with reduced (~10%) uncertainty — reflecting the enriched HPE content of the South China crust.

Geoneutrino Measurement in JUNO

Best fit: 72.6 ± 10.9 TNU (~15% precision)

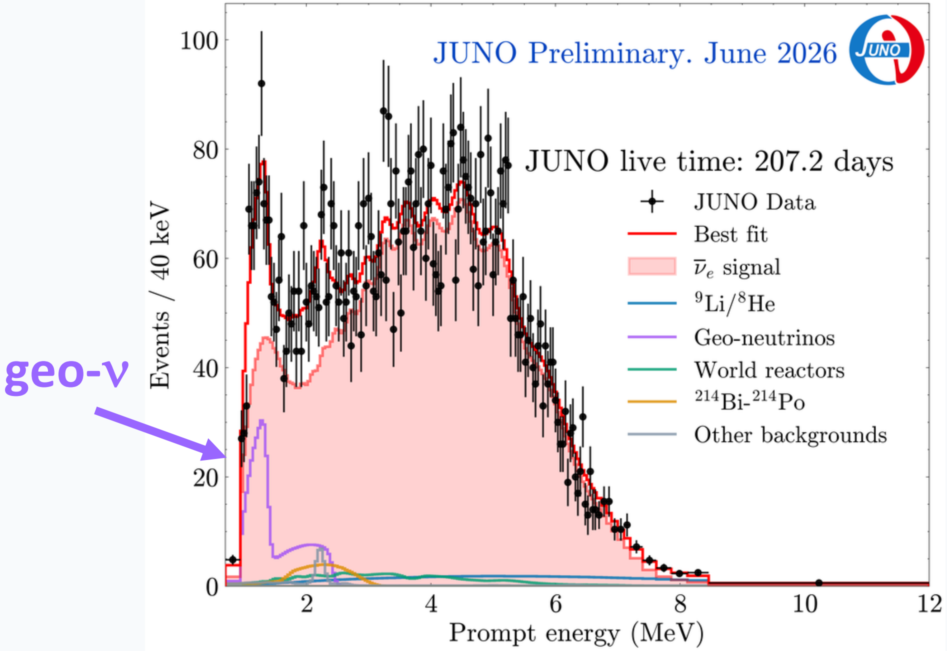

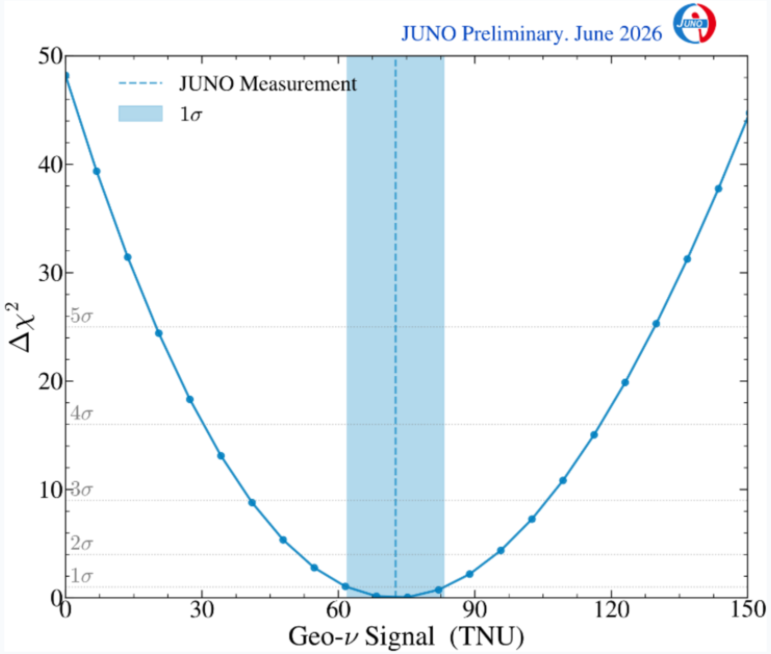

- Fit **without** geo flux constraint
- Th/U signal ratio fixed to chondritic **0.29 (±10%)**
- Zero signal excluded at $> 5\sigma$ ($\Delta\chi^2 > 48$)
- 440 ± 66 geo events from **207.2 days**

Comparing Measurements with Models

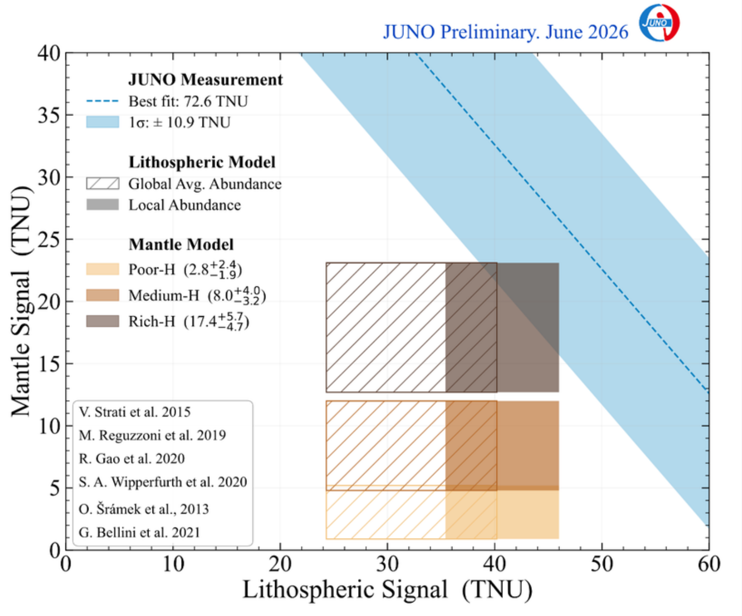

JUNO measurement vs BSE + lithospheric model combinations

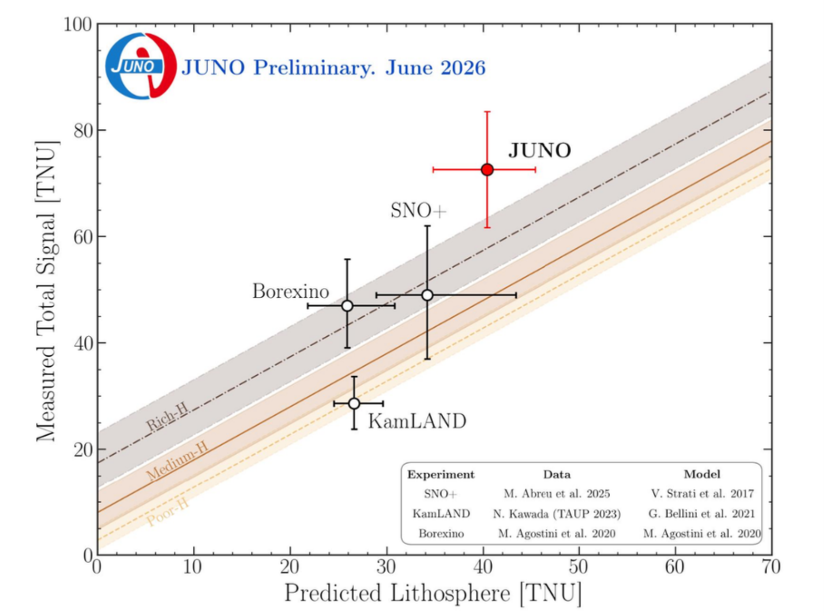

Geoneutrino signals at KamLAND, Borexino, SNO+, JUNO

- JUNO result is **higher than expectation** from existing models, but *not statistically significant*
- Need more JUNO data and more refined geological model predictions

Radiogenic Heat and Mantle Signals

From geoneutrino signal to mantle radiogenic heat

- The expected mantle geoneutrino signal S_M for each BSE class follows a **linear relation** between mantle heat H_M and signal: $S_M = \beta \cdot H_M$, where β depends only on the U/Th spatial distribution in the mantle.
- $S_M = S_{\text{tot}} - S_{\text{LS}}$, and $H_{\text{total}} = H_{\text{LS}} + H_M/[\beta\,(1 - f_K)]$, where $f_K = 0.17$ accounts for the undetectable ^{40}K heat.
- β ranges from **0.75** (HPEs at the core–mantle boundary) to **0.98** (homogeneous mantle), with central value $\beta = 0.86$[1].

> The global surface heat flow is $Q_{\text{surf}} = 47 \pm 2$ **TW**[2]

[1] JUNO Collaboration (T. Adam et al.), "Prospects for geoneutrino detection with JUNO", arXiv:2511.07227 [hep-ex] (2025)
[2] J. H. Davies and D. R. Davies, *Earth's surface heat flux*, Solid Earth 1, 5–24 (2010)

Litho Model	S_{LS} (TNU)	S_M (TNU)	$\beta = 0.75$ (TW)	$\beta = 0.86$ (TW)	$\beta = 0.98$ (TW)
RRM	$30.9^{+6.5}_{-5.2}$	$41.7^{+12.1}_{-12.7}$	$75.1^{+19.5}_{-20.4}$	$66.5^{+17.0}_{-17.8}$	$59.4^{+15.0}_{-15.7}$
GIGJ	$28.9^{+5.5}_{-4.4}$	$43.7^{+11.8}_{-12.2}$	$78.3^{+19.0}_{-19.7}$	$69.3^{+16.6}_{-17.2}$	$61.8^{+14.6}_{-15.1}$
W20 [Crust2.0]	$32.0^{+8.2}_{-6.6}$	$40.6^{+12.7}_{-13.6}$	$73.3^{+20.6}_{-22.0}$	$65.0^{+18.0}_{-19.2}$	$58.0^{+15.8}_{-16.8}$
W20 [Crust1.0]	$31.7^{+8.4}_{-6.6}$	$40.9^{+12.7}_{-13.8}$	$73.8^{+20.6}_{-22.2}$	$65.4^{+18.0}_{-19.3}$	$58.4^{+15.8}_{-17.0}$
W20 [Litho1.0]	$30.7^{+8.1}_{-6.4}$	$41.9^{+12.6}_{-13.6}$	$75.4^{+20.4}_{-21.9}$	$66.8^{+17.8}_{-19.1}$	$59.6^{+15.7}_{-16.8}$
JULOC	$40.4^{+5.6}_{-5.0}$	$32.2^{+12.0}_{-12.3}$	$59.8^{+19.4}_{-19.7}$	$53.2^{+16.9}_{-17.2}$	$47.7^{+14.9}_{-15.1}$
JULOC-I	$41.2^{+4.6}_{-3.3}$	$31.4^{+11.4}_{-11.8}$	$58.5^{+18.4}_{-19.1}$	$52.1^{+16.1}_{-16.6}$	$46.7^{+14.1}_{-14.6}$

Combination of Different Experiments

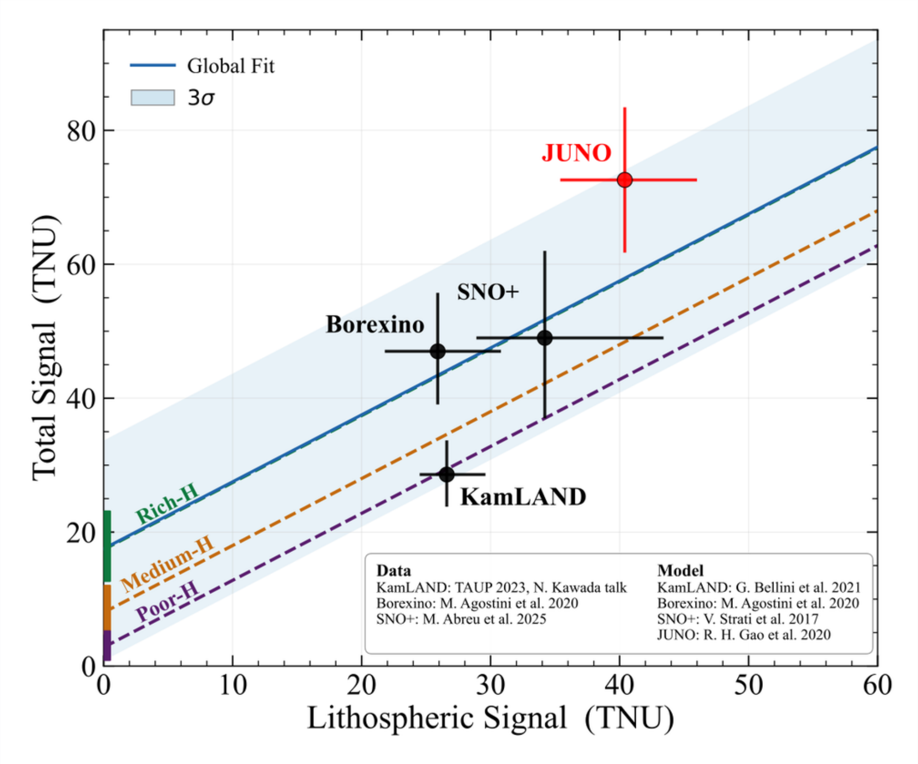

$$17.5^{+5.4}_{-5.6}$$

Best-fit intercept S_{M} (TNU)

- Four experiments: **JUNO + KamLAND + Borexino + SNO+**
- S_{tot} vs predicted S_{LS} at each site
- Unit-slope fit: $S_{\mathrm{tot}} = S_{\mathrm{LS}} + S_{\mathrm{M}}$
- Intercept = **common mantle signal**

Discussion

Interpreting the JUNO measurement

The JUNO measurement ($S_{\mathrm{tot}} = 72.6 \pm 10.9$ TNU) is **higher than most model predictions** (~ 32–59 TNU range) .

Possible explanations

- **Local crust model** — JULOC may underestimate the HPE content of the South China crust
- **CLM Th/U ratio** — Continental Lithospheric Mantle beneath South China may be enriched relative to the chondritic value adopted in current models
- **Mantle heterogeneity** — JUNO site may not represent the global average
- **Data fluctuation or unknown backgrounds?**

- No definitive conclusion at this stage
- More JUNO data needed to reduce statistical uncertainty
- Refined geological models (especially local crust) are essential

Summary

Oscillation & NMO

Precision of solar oscillation parameters further improved by **a factor of 1.3–1.5**

First measurement on Δm^2_{31} achieved a precision of **~1%**

With external constraint, **Normal Mass Ordering** is favored at **~2.3σ**

Geoneutrino Measurement

$S_{\rm tot}(\mathrm{U{+}Th}) = 72.6 \pm 10.9$ **TNU**

from **207.2 days** of JUNO data

440 ± 66 geoneutrino candidates

$> 5\sigma$ detection significance

More data needed to constrain geo-models

JUNO opens a new era of precision geoneutrino physics.